◻   84

Verification of Quartz Crystal Microbalance Array Using Vector Network Analyzer and OpenQCM

**Ahmad Anwar Zainuddin[1], Anis Nurashikin Nordin[2] , Rosminazuin Ab. Rahim[3],
Aliza Aini Md. Ralib[4], Sheroz Khan[5], Cyril Guines[6], Matthieu Chatras[7], Arnaud Pothier[8]**
[1,2,3,4,5] Department of Electrical and Computer Engineering, Kulliyyah of Engineering,
International Islamic University Malaysia, Kuala Lumpur, Malaysia
[6,7,8] XLIM Research Institute, UMR CNRS 7252 Université de Limoges, Limoges Cedex, France

ABSTRACT

Quartz Crystal Microbalance (QCM) is a device that allows non-destructive measurements of r in situ reaction activities. In this article, an array comprising of six 3MHz QCM sensors in an array were characterized using a vector network analyzer and OpenQCM, a portable measuring instrument that measures change in resonance frequency. Measurements of S21 transmission characteristics using the vector network analyzer provides the resonance frequency and can also be used to derive the RLC equivalent electrical circuit values of a resonant two-port network based on the Butterworth-Van Dyke model. In this work, R_m, L_m, C_m and C_o were obtained via curve-fitting of the measurement results to the simulated results. Measurements were done in triplicates to verify reproducibility for all 6 sensors. For comparison, measurements were also done using a portable, open-source instrument, OpenQCM. The OpenQCM instrument directly measures changes in resonance frequencies, making it ideal for biosensing experiments, which correlate changes in mass with changes in resonance frequencies. Comparison between resonance frequency measurements using VNA and OpenQCM exhibit low percentage difference 0.2%. This QCM sensor array has the potential of conducting real-time, point-of-care analyses for detection of biological molecules.

Corresponding Author:

Anis Nurashikin Nordin,
Department of Electrical and Computer Engineering, Kulliyyah of Engineering,
International Islamic University Malaysia,
Kuala Lumpur, Malaysia.
Email: anisnn@iium.edu.my

1.   INTRODUCTION

Over the past two decades, intensive research on biosensors have been carried out in the development of label-free quantification and point-of-care medical diagnostics [1]–[4]. Biosensors can be defined as analytical devices that capture biological responses associated with a particular disease (bio-recognition element) in the form of detectible electrical signals (transduction method). Some typical examples of bio-recognition elements are cells, enzymes, biomolecules, aptamers, and antibodies [5]. The transduction method can translate these bio-recognition elements into quantifiable signals. Several types of transducers have been employed over the years as biosensors; e.g. electrochemical [6],[7], mass-sensing (mechanical) [8],[9], optical [10],[11], and field-effect transistors [12].

There is an increasing demand for specific, low cost, portable and highly sensitive biosensors. Point-of-care (POC) biosensor systems provides a comprehensive solution as it provides label free detection, real-time monitoring, that is easily portable which is also relatively cheap [1],[13]–[22]. Technically, POC devices can be classified as portable systems that are separate from other miniaturized platforms due to their

ability to perform analyses in the field. These systems can also be implemented such that it integrates with the multiple existing lab processes using microfluidic systems that allows detection using various types of transduction methods and real-time result acquisitions [23].

Among the different types of transduction methods, optical methods such as surface-plasmon resonance or SPR, fluorescence, and optical cavity resonators were reported to be some of the most sensitive [10],[11],[21]. SPRs measure surface-based chemical reactions that correspond to refractive index changes, thus giving change to the optical signal. SPRs are however, impractical for POC applications due to its expensive equipment which also require specific technical expertise to operate [13]. Recent work have shown interest on analyses of other transduction methods such as electrochemical detection and mass-sensing. These methods have exhibited several advantages for instance, ease of operation, low cost, and minimal operating procedures [6]-[9]. Furthermore, electrochemical detection like electrochemical impedance spectroscopy (EIS) and cyclic voltammetry (CV) utilizes screen printed electrodes (SPEs) which are commonly used in the biosensing field [24]–[28]. This method detects impedance or current changes in electrode surface owing to transport or surface reactions [23]. However, this method is principally categorized as a destructive process since it applies direct current (DC) and alternate current (AC) through a system, hence deteriorating the electrode surface, specifically in SPE applications. Although the permanent change on the electrode surface is in nano-range scale, it still destabilizes the current or impedance of the system. Hence, non-uniform results are observable if the same SPE is used in another application. For this reason, most SPEs are disposable, where the electrodes are only meant for single-use applications for specific target detection and specific transduction methods like EIS and CV [29]. Although SPEs are low-cost POC devices, it will increase operational cost and time especially when it involves establishing multiple testing or results verification.

Apart from the electrochemical methods, mass-sensing or Quartz Crystal Microbalance sensors (QCMs) are also widely used as it is a non-destructive and ultrasensitive sensor. These sensors only apply very low amplitude alternate currents (AC) to the top and bottom electrode surfaces of piezoelectric substrates, typically AT-cut Quartz crystals. This results in a substantially low current being applied to measure the chemical interactions on the electrode's surface without physically modifying it, ensuring longer usage and reproducibility of results. For certain experiments, QCMs can also be cleaned using chemistry solutions or ultrasonic treatment, allowing it to be reused. Due to this, QCMs have been widely used for biochemistry detection [30]–[37]. QCM sensors can evaluate the changes in mass and density-viscosity of complex biological responses on the surface of its crystal sensor based on changes in the resonance frequency [38]. The resonance frequency of the propagating acoustic wave through the surface of the quartz will reduce due to mass change [39]–[41]. In most common cases, these sensors can even detect frequency shifts of 1 Hz by using high frequency oscillators (in the MHz range) [42] allowing it to detect masses in the sub-ng level. The QCMs generally have low spurious bulk signals and good temperature stability. The wave mode in a QCM is bulk thickness shear mode (TSM), which allows for operation in both dry and liquid environments. The mass-sensing method has been used (via Sauerbrey theory) in various fields such as environmental analyses, security monitoring, food safety and medical diagnostics [31],[43].

In recent years, an increasing amount of literature has been reported on the development of QCM arrays in biosensing applications [44]–[46]. These works aid users to execute parallel and simultaneous multi-target analyses. It will significantly simplify tedious procedures of manipulating concentrations, data range, and different target molecules by having multiple arrays on a single disk. Furthermore, it can be integrated with microfluidic systems for continuous real-time experiments without significant error in quality factor [44]. A QCM that operates in aqueous environment can detect density-viscosity and acoustic impedance effects, making it a highly sensitive device. Placement of several QCMs in an array allow multiple parallel measurements, improving the throughput of the device. Arrangement of these sensors in array need to take into consideration several aspects such as cross-talk between sensors, energy loss due to liquid damping and other factors [47]–[49]. One key point for the design of these sensors is that the Q-factor of each sensor has to be high to overcome liquid damping. An optimal gap between the sensors is also necessary to avoid frequency interference, hence decreasing the Q-factor error for each sensor.

This paper focuses on the simulation and verification of the QCM array using vector network analyzer (VNA) and an open source portable measuring instrument, (OpenQCM). In this work, we simulate and fabricate six 3MHz of QCM sensors on a single wafer. Design details of the QCM have been reported previously in [50]. Initially, a classical Butterworth-van-Dyke (BVD) model was used to calculate the impedance parameters (RLC) of each QCM sensor. The results were then used to simulate a resonance frequency analyses using ADS software. Comparison between the theoretical and experimental resonance frequency analyses was performed next. This report is organized into six sections with the first section introducing the biosensor and the significance of POC in diagnostic applications. Section 2 comprises the underlying theories behind the proposed QCM sensor as Section 3 deals with the ADS simulation model. The

measurement settings are described in Section 4. Meanwhile, all calculations and related measurement results are presented in Section 5. Section 6 states the conclusions made from this research.

2.   BIOSENSOR PRINCIPLES AND DESIGN THEORY
2.1. Device structure

Figure 1 shows the top and cross sectional views of the device together and operation as a mass sensor. This biosensor comprises two deposited metal on the top and bottom of a quartz crystal. The variables r and s indicate the radius of working electrode and centre-to-centre distance of two adjacent QCM sensors, respectively. The diameter of quartz substrate is 76mm, quartz thickness, h = 500µm and sensor radius, r = 3.30mm were used in this work. The centre-to-centre distance of QCM, s is was set to 6mm to minimize frequency interference.
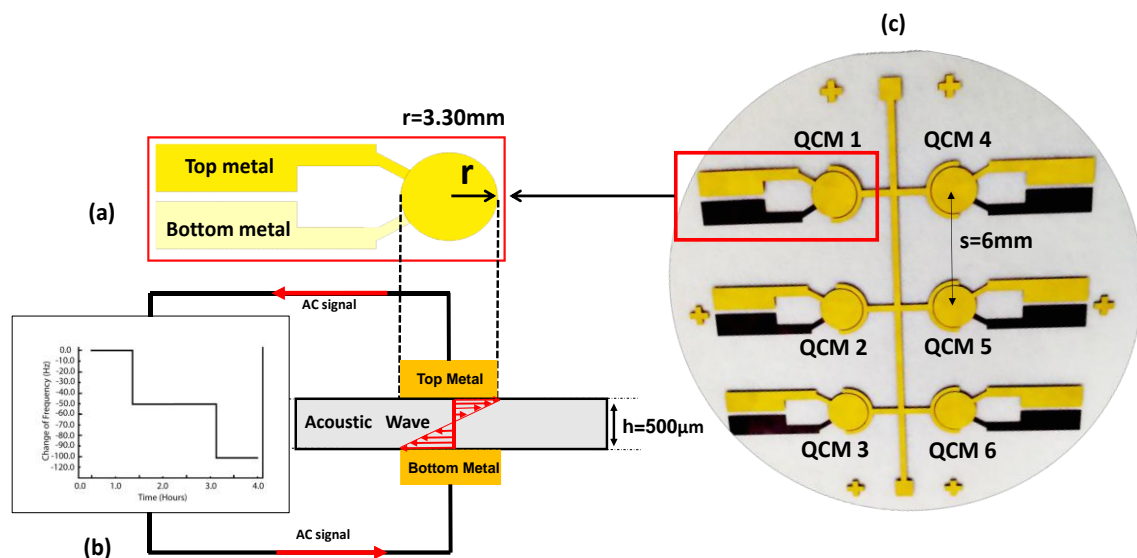
Figure 1. (a) Design geometry of a single QCM sensor (b) Operation as a mass sensor (c) QCM array

An AC signal is applied between the top and bottom AT-quartz electrodes to generate acoustic wave energy and produce resonance. When used for biosensing applications, frequency shifts will be induced when biological materials are placed on the top electrode due to additional mass. Placement of six sensors in an array allows multiple detection in a single platform.

2.2. Equivalent circuit models

The QCM can be electrically represented using an equivalent circuit based on the classical Butterworth-van-Dyke (BVD) circuit as shown in Figure 2 [51]-[52]. This theory is established from a one-dimensional analyses of a piezoelectric resonator as described in [52].
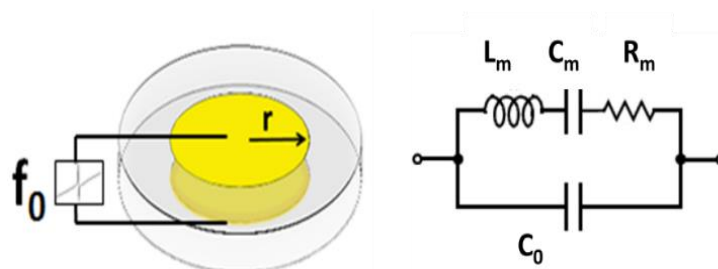
Figure 2. The Butterworth Van Dyke (BVD) electrical equivalent circuit as a QCM model in air conditions

The RLC parameters of the equivalent circuit can be divided into motional components, R_m, L_m and C_m which are derived from the resonance operation of the QCM and an additional parallel static capacitor (C_0). This additional C_0 contributes to the dielectric energy storage because the oscillation crystal is established in between the two electrodes. The motional resistance, R_m represents dissipation or energy loss during resonance. The motional impedance, L_m and motional capacitance, C_m correspond to the mass of the resonator and coupling coefficient, respectively. The equations for these motional elements are as expressed in Eq. (1)-(4). Table 1 summarizes the material properties used to perform this calculation.

$$C_0 = \frac{\varepsilon_{22}\pi r^2}{d_q} \tag{1}$$

$$C_m = \frac{8K_0^2 \varepsilon_{22}\pi r^2}{d_q(N\pi)^2} \tag{2}$$

$$L_m = \frac{1}{\omega_S^2 C_m} \tag{3}$$

$$R_m = \frac{\eta_q}{\bar{c}_{66} C_m} \tag{4}$$

Table 1. Material properties used in the calculation and ADS simulation

Parameters	Values	Unit	Ref.
ρ_q, Density of quartz	2.648×10^3	kgm^{-3}	[54]
μ_q, Shear modulus of quartz	2.947×10^{10}	Pa or Nm^{-2}	[54]
ρ_l, Density of liquid (water)	1×10^3	kgm^{-3}	[55]
η_l, Viscousity of liquid, Pa.s	1×10^{-4}	Pa.s	[56]
μ_l, Shear modulus of liquid (water)	2.3×10^{-9}	Pa or Nm^{-2}	[57]
μ_f, Shear modulus of film (gold)	2.6×10^{-10}	Pa or Nm^{-2}	COMSOL
ρ_f, Density of film(gold)	193×10^3	kgm^{-3}	COMSOL
ε_{22}, Quartz permittivity	3.98×10^{-11}	A^2.s^4.Kg^{-1}.m^{-3}	[58]
ρ_q, Piezoelectric constant of quartz	9.65×10^{-2}	A.s.m^{-2}	[59]
K_0^2, electromechanical coupling constant	7.74×10^{-3}	Pa or Nm^{-2}	[50],[60]
η_q, Quartz viscosity	0.42	Pa.s	[58]

3. EXTRACTION AND SIMULATION OF RLC EQUIVALENT CIRCUIT

In this section, a computer-aided synthesis program (ADS software) was used in order to determine the RLC equivalent circuit parameters of the QCM sensor. The calculated values of RLC parameters are predicted using Equation (1)-(4) as described in Section 2. The RLC equivalent circuit is next simulated using ADS in a two-port network to obtain its S21 or transmission parameters. Figure 3 shows the S2p simulation setup in which port 1 and port 2 correspond to input and output ports, respectively. An AC frequency domain analysis is done from 2.77MHz to 3.77MHz. A step size of 5kHz is set to obtain high-accuracy simulations. Tuning and optimization methods are done next to extract relevant physical parameters. The simulation results are compared and tuned to experimental measurement results to obtain the RLC parameters of the QCM sensor.
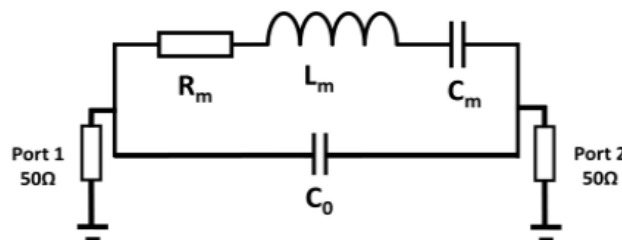
Figure 3. S2p simulation setup via ADS software

4. EXPERIMENTAL WORK

In this section, two different equipments were used to measure the resonance frequency of the QCM array. In the first experiment the QCM sensors were measured using a vector network analyzer (VNA),

Agilent E5061A. In the second experiment, the OpenQCM device was used to measure the resonance frequency. The OpenQCM is essentially an Arduino microcontroller having ATMega32U4 processor with 16 MHz clock speed. The frequency of the vibrating quartz crystal was measured using the FreqCount algorithm developed by Paul Stoffregen from PJRC. The software on the OpenQCM is open source and can be customized for different applications. The main motivation to utilize the OpenQCM, is its portability and its ease of use compared to VNAs, which are unsuitable for field measurements and require additional data processing for mass measurements. Usage of OpenQCM does have some limitations however, as it can only detect QCMs with resonance Qs of larger than 1000.

4.1. Measurements using Vector Network Analyzer

Figure 4 shows the connection setup of the QCM array to the VNA via a printed circuit board (PCB). The PCB was fabricated with the input and output ports that uses two SMA connectors. Short 3-cm wires were soldered at both input and output ports to enable a connection to the QCM sensor using clip connectors. In order to obtain high-accuracy measurements, AC frequency domain analyses were set from 2.77MHz to 3.77MHz with a step size of 5kHz.
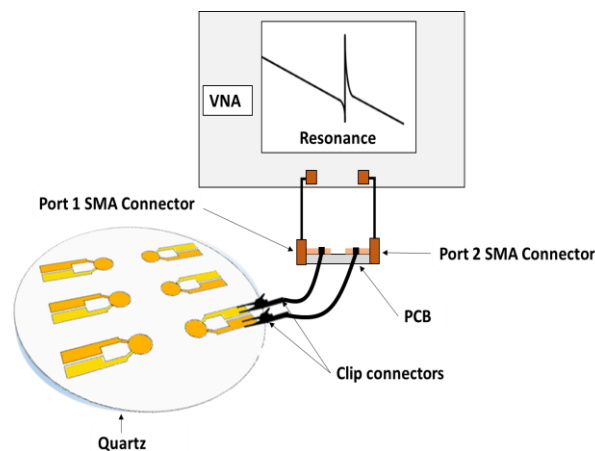
Figure 4. Experimental setup of for measurements using Vector Network Analyzer

4.2. Measurements using OpenQCM

Figure 5 indicates the experimental setup of the QCM sensor array using the OpenQCM device. The input and output ports were connected via direct clip connectors. The OpenQCM device was connected to the computer using a USB connector. The measurement records the QCM's resonance frequency, duration of the experiment and the current temperature. In this work, the duration was set to 300s in order allow sufficient time for each QCM to achieve stable resonances before the measurements are recorded.
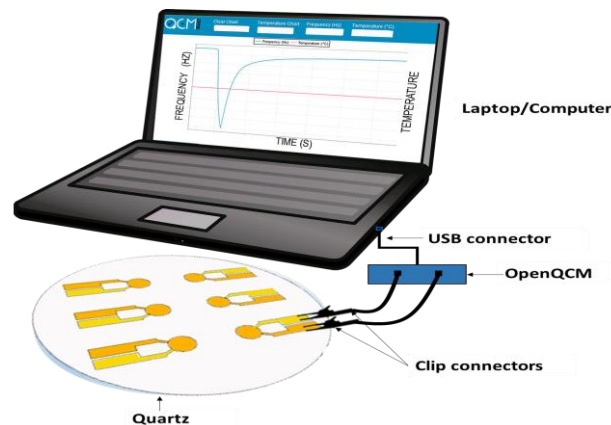
Figure 5. A connection setup of OpenQCM measurement

5. RESULT AND ANALYSES

5.1. Resonance frequency analyses using VNA and extrated RLC parameters

Figure 6 shows the measured resonances for QCM1, QCM3 and QCM6. Measurements were done in triplicates for each QCM. Measurement results are reproducible. The average resonance frequency of 3.281MHz ± 0.004MHz was recorded in this work.

(a)

(b)

(c)
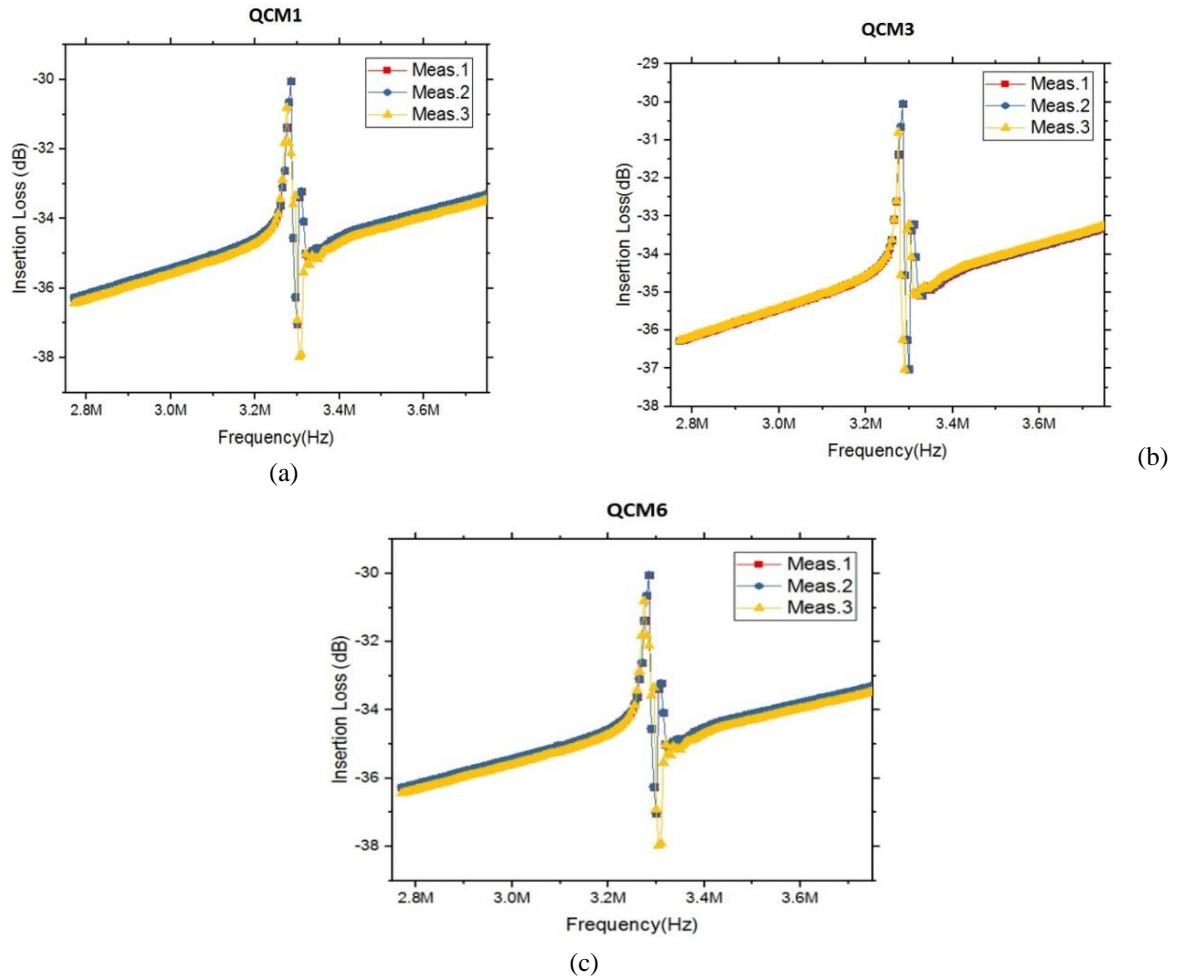
Figure 6. The triplicate S21 transmission characteristics resonance frequency measurements (a) QCM1 (b) QCM3 and (c)QCM 6 using VNA

Based on the experimental measurements, ADS simulation of the 2-port network shown in Figure 3 can be used to obtain the extracted equivalent circuit parameters. Figure 7 shows the both the simulated ADS and measured S21 transmission characteristics. From the graph, it can be seen that both results are in good agreement with a resonance frequency of close to 3.281MHz. The extracted equivalent circuit parameters are detailed in Table 2.

Table 2. QCM measured performance and extracted equivalent circuit parameters

Measured		Extracted			
Resonance frequency (MHz)	Q-factor	R_m(kΩ)	C_0(pF)	L_m(H)	C_m(fF)
3.281	141	4.701	9.991	0.136	17.200
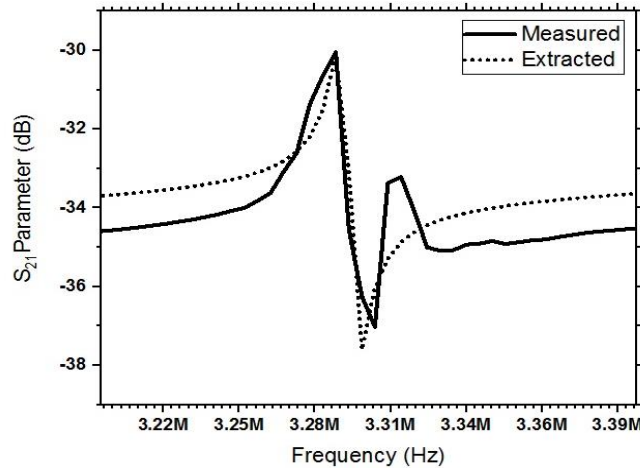
Figure 7. S_{21} Magnitude Transmission characteristics of QCM

Measured graph obtained from measurements using the experimental setup shown in Figure 5. Extracted characteristics were simulated using the calculated values shown in Table 2 via Equation (1-)(4) and next fine-tuned to match the measurement results.

5.2. Resonance frequency analyses using OpenQCM device

Figure 8 shows the experimental results for all QCMs. From the results, a stable transmission frequency of 3.290±0.004MHz for 6 QCMs array in a constant temperature of 31℃. These results complied with the resonance frequency measurement using VNA with only a small tolerance of 0.3% and 0.4% respectively. Table 3 summarizes the analyses of resonance frequency measurement in terms of theoretical and experimental methods as discussed previously in this section.
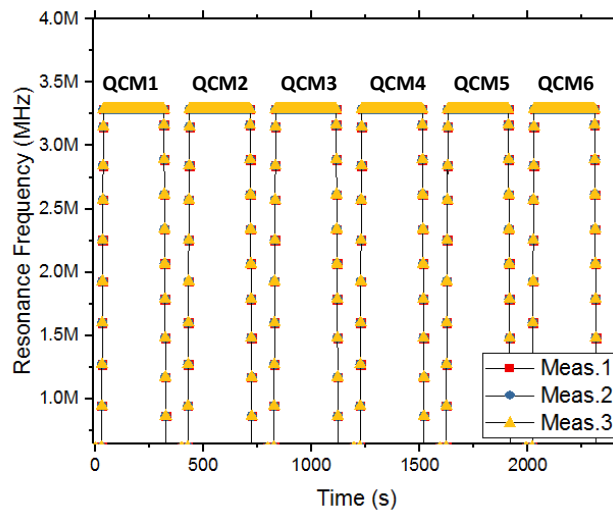
Figure 8. The triplicate resonance frequency measurements for all QCMs via OpenQCM device

Table 3. Comparison of resonance frequency measurements using VNA and OpenQCM

QCM	Measurement,VNA (MHz),F_{0M}	Measurement,OpenQCM (MHz)	Difference VNA Vs. QCM (%)
QCM1	3.281±0.005	3.289±0.004	0.223
QCM2	3.278±0.005	3.287±0.004	0.270
QCM3	3.281±0.004	3.289±0.004	0.224
QCM4	3.278±0.005	3.287±0.004	0.259
QCM5	3.281±0.004	3.289±0.004	0.224
QCM6	3.281±0.005	3.289±0.004	0.222

6.   CONCLUSION

An array of biosensors comprising of 6 QCMs on a single wafer have been fabricated and characterized in this work. Measurements were done using both a vector network analyzer (VNA) and a portable instrument, OpenQCM have been discussed. Measurements of S21 transmission characteristics using the VNA can also be used to determine the RLC equivalent electrical circuit values of R_m, L_m, C_m and C_o. Measurements were done in triplicates to verify reproducibility for all 6 sensors. Next, measurements using a portable, open-source instrument, OpenQCM were made. The OpenQCM instrument directly measures changes in resonance frequencies, making it ideal for biosensing experiments, which correlate changes in mass with changes in resonance frequencies. Comparison between resonance frequency measurements using VNA and OpenQCM exhibit low percentage difference 0.2%. This sensor has the potential of real-time analyses and parallel monitoring or detection of biological molecules. When integrated with the OpenQCM, this sensor has the potential of performing on the field analyses due to its portability and ease of use.

REFERENCES

[1]   S. John A. and Price C. P., "Existing and emerging technologies for point-of-care testing," *Clin Biochem Rev.*, vol/issue: 35(3), pp. 155, 2014.
[2]   Lisowski P. and Zarzycki P. K., "Microfluidic paper-based analytical devices (μPADs) and micro total analyses systems (μTAS): development, applications and future trends," *Chromatographia,* vol/issue: 76(19–20), pp. 1201–1214, 2013.
[3]   King K.R., *et al.*, "Point-of-Care Technologies for Precision Cardiovascular Care and Clinical Research," *JACC Basic Transl Sci.*, vol/issue: 1(1–2), pp. 73–86, 2016.
[4]   Hu J., *et al.*, "Portable microfluidic and smartphone-based devices for monitoring of cardiovascular diseases at the point of care," *Biotechnol Adv.*, vol/issue: 34(3), pp. 305–320, 2016.
[5]   Silva E. T., *et al.*, "Electrochemical biosensors in point-of-care devices: recent advances and future trends," *Chem Electro Chem,* 2017.
[6]   Darwish N. T., *et al.*, "Electrochemical Immunosensor Based on Antibody-Nanoparticle Hybrid for Specific Detection of the Dengue Virus NS1 Biomarker," *J Electrochem Soc.*, vol/issue: 163(3), pp. B19–25, 2016.
[7]   Zainuddin A. A., *et al.*, "Modeling of a novel biosensor with integrated mass and electrochemical sensing capabilities," *2016 IEEE EMBS Conference on Biomedical Engineering and Sciences (IECBES),* pp. 420–5, 2016.
[8]   Ziegler C., "Cantilever-based biosensors," *Anal Bioanal Chem,* vol/issue: 379(7–8), pp. 946–959, 2004.
[9]   Janshoff A., *et al.*, "Piezoelectric Mass-Sensing Devices as Biosensors—an Alternative to Optical Biosensors?" *Angew Chem Int Ed.*, vol/issue: 39(22), pp. 4004–4032, 2000.
[10]   Han M., *et al.*, "Quantum-dot-tagged microbeads for multiplexed optical coding of biomolecules," *Nat Biotechnol.*, vol/issue: 19(7), pp. 631, 2001.
[11]   Fan X., *et al.*, "Sensitive optical biosensors for unlabeled targets: A review," *Anal Chim Acta,* vol/issue: 620(1), pp. 8–26, 2008.
[12]   Zheng G., *et al.*, "Multiplexed electrical detection of cancer markers with nanowire sensor arrays," *Nat Biotechnol.*, vol/issue: 23(10), pp. 1294, 2005.
[13]   Verrastro M., *et al.*, "Amperometric biosensor based on Laccase immobilized onto a screen-printed electrode by Matrix Assisted Pulsed Laser Evaporation," *Talanta*, vol. 154, pp. 438–445, 2016.
[14]   E. Harrad L. and Amine A., "Amperometric biosensor based on prussian blue and nafion modified screen-printed electrode for screening of potential xanthine oxidase inhibitors from medicinal plants," *Enzyme Microb Technol.*, vol. 85, pp. 57–63, 2016.
[15]   Silva B. V. M., *et al.*, "An ultrasensitive human cardiac troponin T graphene screen-printed electrode based on electropolymerized-molecularly imprinted conducting polymer," *Biosens Bioelectron,* vol. 77, pp. 978–85, 2016.
[16]   Salam F. and Tothill I. E., "Detection of Salmonella typhimurium using an electrochemical immunosensor," *Biosens Bioelectron,* vol/issue: 24(8), pp. 2630–2636, 2009.
[17]   Zhybak M. T., *et al.*, "Direct detection of ammonium ion by means of oxygen electrocatalysis at a copper-polyaniline composite on a screen-printed electrode," *Microchim Acta,* vol/issue: 183(6), pp. 1981–7, 2016.
[18]   Arduini F., *et al.*, "Electrochemical biosensors based on nanomodified screen-printed electrodes: Recent applications in clinical analyses," *TrAC Trends Anal Chem.*, vol. 79, pp. 114–26, 2016.
[19]   Zhu Y., *et al.*, "Label-free detection of kanamycin based on the aptamer-functionalized conducting polymer/gold nanocomposite," *Biosens Bioelectron,* vol/issue: 36(1), pp. 29–34, 2012.
[20]   Zelada G. G. A., *et al.*, "Label-free detection of Staphylococcus aureus in skin using real-time potentiometric biosensors based on carbon nanotubes and aptamers," *Biosens Bioelectron,* vol/issue: 31(1), pp. 226–232, 2012.

[21]   Fernández E., *et al.*, "Mercury determination in urine samples by gold nanostructured screen-printed carbon electrodes after vortex-assisted ionic liquid dispersive liquid–liquid microextraction," *Anal Chim Acta,* vol. 915, pp. 49–55, 2016.

[22]   Rebelo T. S., *et al.*, "Protein imprinted materials designed with charged binding sites on screen-printed electrode for microseminoprotein-beta determination in biological samples," *Sens Actuators B Chem.*, vol. 223, pp. 846–852, 2016.

[23]   Prakash S., *et al.*, "Theory, fabrication and applications of microfluidic and nanofluidic biosensors," *Phil Trans R Soc A*, vol/issue: 370(1967), pp. 2269–2303, 2012.

[24]   Hayat A. and Marty J. L., "Disposable screen printed electrochemical sensors: Tools for environmental monitoring," *Sensors*, vol/issue: 14(6), pp. 10432–10453, 2014.

[25]   Amin S., *et al.*, "Disposable screen printed graphite electrode for the direct electrochemical determination of ibuprofen in surface water," *Environ Nanotechnol Monit Manag*., vol. 1, pp. 8–13, 2014.

[26]   Taleat Z., *et al.*, "Screen-printed electrodes for biosensing: a review (2008–2013)," *Microchim Acta,* vol/issue: 181(9–10), pp. 865–891, 2014.

[27]   Balkenhohl T. and Lisdat F., "Screen-printed electrodes as impedimetric immunosensors for the detection of anti-transglutaminase antibodies in human sera," *Anal Chim Acta,* vol/issue: 597(1), pp. 50–57, 2007.

[28]   Alonso L. M. A., *et al.*, "Screen-printed biosensors in microbiology; a review," *Talanta,* vol/issue: 82(5), pp. 1629–1636, 2010.

[29]   Zainuddin A. A., *et al.*, "Modeling of a novel biosensor with integrated mass and electrochemical sensing capabilities," *Biomedical Engineering and Sciences (IECBES), 2016 IEEE EMBS Conference on*, pp. 420–425, 2016.

[30]   Lu F., *et al.*, "Energy-trapping analyses for the bi-stepped mesa quartz crystal microbalance using the finite element method," *Smart Mater Struct*., vol/issue: 14(1), pp. 272, 2005.

[31]   Nordin A. N., *et al.*, "Screen Printed Electromechanical Micro-total Analyses System (µtas) for Sensitive and Rapid Detection of Infectious Diseases," *Procedia Technol*., vol. 27, pp. 100–101, 2017.

[32]   Kao W. L., *et al.*, "Effect of Surface Potential on the Adhesion Behavior of NIH3T3 Cells Revealed by Quartz Crystal Microbalance with Dissipation Monitoring (QCM-D)," *J Phys Chem C*, vol/issue: 121(1), pp. 533–541, 2017.

[33]   Martin S. J., *et al.*, "Characterization of a quartz crystal microbalance with simultaneous mass and liquid loading," *Anal Chem.*, vol/issue: 63(20), pp. 2272–2281, 1991.

[34]   March C., *et al.*, "High-frequency phase shift measurement greatly enhances the sensitivity of QCM immunosensors," *Biosens Bioelectron,* vol. 65, pp. 1–8, 2015.

[35]   Hieda M., *et al.*, "Ultrasensitive quartz crystal microbalance with porous gold electrodes," *Appl Phys Lett.*, vol/issue: 84(4), pp. 628–630, 2004.

[36]   Peng H. B., *et al.*, "Ultrahigh frequency nanotube resonators," *Phys Rev Lett.*, vol/issue: 97(8), pp. 087203, 2006.

[37]   Lu F., *et al.*, "Quartz crystal microbalance with rigid mass partially attached on electrode surfaces," *Sens Actuators Phys*., vol/issue: 112(2), pp. 203–210, 2004.

[38]   Voiculescu I. and Nordin A. N., "Acoustic wave based MEMS devices for biosensing applications," *Biosens Bioelectron,* vol/issue: 33(1), pp. 1–9, 2012.

[39]   Jacobs J., "Converters in Biology," *Biomechanics and Related Bio-Engineering Topics: Proceedings of a Symposium Held in Glasgow*, pp. 63, 1964.

[40]   Kim B. C., *et al.*, "In-Line Measurement of Water Contents in Ethanol Using a Zeolite-Coated Quartz Crystal Microbalance," *Sensors,* vol/issue: 15(10), pp. 27273–27282, 2015.

[41]   Fu Y. Q., *et al.*, "Piezoelectric Zinc Oxide and Aluminum Nitride Films for Microfluidic and Biosensing Applications," *Biol Biomed Coat Handb Appl.*, pp. 335, 2016.

[42]   Lucklum R. and Hauptmann P., "The Δf–ΔR QCM technique: an approach to an advanced sensor signal interpretation," *Electrochimica Acta,* vol/issue: 45(22), pp. 3907–16, 2000.

[43]   Turner N. W., *et al.*, "The use of a quartz crystal microbalance as an analytical tool to monitor particle/surface and particle/particle interactions under dry ambient and pressurized conditions: a study using common inhaler components," *Analyst*, vol/issue: 142(1), pp. 229–236, 2017.

[44]   Liu F., *et al.*, "A novel cell-based hybrid acoustic wave biosensor with impedimetric sensing capabilities," *Sensors,* vol/issue: 13(3), pp. 3039–3055, 2013.

[45]   Dunham G. C., *et al.*, "Dual quartz crystal microbalance," *Anal Chem,* vol/issue: 67(2), pp. 267–272, 1995.

[46]   Bruckenstein S., *et al.*, "Dual quartz crystal microbalance compensation using a submerged reference crystal. Effect of surface roughness and liquid properties," *J Electroanal Chem.*, vol/issue: 370(1–2), pp. 189–195, 1994.

[47]   Kankare J., "Sauerbrey equation of quartz crystal microbalance in liquid medium," *Langmuir,* vol/issue: 18(18), pp. 7092–7094, 2002.

[48]   Michalzik M., *et al.*, "Miniaturized QCM-based flow system for immunosensor application in liquid," *Sens Actuators B Chem.*, vol. 111, pp. 410–415, 2005.

[49]   Dunham G. C., *et al.*, "Dual quartz crystal microbalance," *Anal Chem.*, vol/issue: 67(2), pp. 267–272, 1995.

[50]   Zainuddin A. A., *et al.*, "Design and Optimization of a MEMS Quartz Mass Sensor Array for Biosensing," in *2017 IEEE International Conference on Smart Instrumentation, Measurement and Applications (ICSIMA), Kuala Lumpur*, 2017.

[51]   Baron T., *et al.*, "A pressure sensor based on a HBAR micromachined structure," *2010 IEEE International Frequency Control Symposium,* pp. 361–4, 2010.

[52] Granstaff V. E. and Martin S. J., "Characterization of a thickness-shear mode quartz resonator with multiple nonpiezoelectric layers," *J Appl Phys.*, vol/issue: 75(3), pp. 1319–1329, 1994.

[53] Tsai Y. J., *et al.*, "Robust design of quartz crystal microbalance using finite element and Taguchi method," *Sens Actuators B Chem.*, vol/issue: 92(3), pp. 337–344, 2003.

[54] Wu H., *et al.*, "Real-Time Monitoring of Platelet Activation Using Quartz Thickness-Shear Mode Resonator Sensors," *Biophys J.*, vol/issue: 110(3), pp. 669–679, 2016.

[55] Venkateswara R. A., *et al.*, "Transport of liquids using superhydrophobic aerogels," *J Colloid Interface Sci.*, vol/issue: 285(1), pp. 413–8, 2005.

[56] Beece D., *et al*., "Solvent viscosity and protein dynamics," *Biochemistry (Mosc),* vol/issue: 19(23), pp. 5147–5157, 1980.

[57] Yamamoto T., "Acoustic propagation in the ocean with a poro-elastic bottom," *J Acoust Soc Am.*, vol/issue: 73(5), pp. 1587–96, 1983.

[58] Arnau A., "Piezoelectric transducers and applications," Springer, 2004.

[59] Carr P. H., "Measurement of the piezoelectric constant of quartz at gigacycle frequencies," *J Acoust Soc Am.*, vol/issue: 41(1), pp. 75–83, 1967.

[60] Zhang J., *et al.*, "Antibody/antigen affinity behavior in liquid environment with electrical impedance analyses of quartz crystal microbalances," *Biophys Chem*., vol/issue: 99(1), pp. 31–41, 2002.